Coupled-cluster calculations for the ground and excited states of the spin-half *XXZ* model

2011 J. Phys.: Condens. Matter 23 406001

(http://iopscience.iop.org/0953-8984/23/40/406001)

J. Phys.: Condens. Matter **23** (2011) 406001 (7pp) doi:10.1088/0953-8984/23/40/406001

Coupled-cluster calculations for the ground and excited states of the spin-half *XXZ* model

Mohammad Merdan and Y Xian

School of Physics and Astronomy, The University of Manchester, Manchester M13 9PL, UK

Received 29 June 2011, in final form 22 August 2011
Published 21 September 2011
Online at stacks.iop.org/JPhysCM/23/406001

Abstract
The coupled-cluster method is applied to the spin-1/2 antiferromagnetic *XXZ* model on a square lattice by employing an approximation which contains two-body long-range correlations and high-order four-body local correlations. Improvement is found for the ground-state energy, the sublattice magnetization and the critical anisotropy when comparing with the approximation including the two-body correlations alone. We also obtain the full excitation spectrum which is in good agreement with the quantum Monte Carlo results and the high-order spin-wave theory.

(Some figures in this article are in colour only in the electronic version)

1. Introduction

The coupled-cluster method (CCM) is one of the most precise microscopic formulations of quantum many-body theories [1–9]. There have been a large number of successful applications of the CCM to a wide range of physical and chemical systems. In particular, the applications of the CCM to spin systems on discrete spatial lattices have produced one of the most accurate results [10–20]. Several approximation schemes have been developed for the application of the CCM to the spin–lattice systems. Two such successful schemes are the so-called SUBn scheme in which all correlations of any range for up to n spins are retained and the localized LSUBm scheme in which m or fewer adjacent spin sites over all distinct locales on the lattice are retained. Other high-order localized approximation schemes such as DSUBm [19] and LPSUBm [20] have also been employed. Up to now, most recent studies have presented results for the high-order calculations mainly based on the LSUBm scheme in which the long-range-order correlations are ignored [13–20]. In this paper we present results for the ground and excitation states for an antiferromagnetic square lattice by combining the SUB2 and LSUB4 approximation schemes (SUB2+LSUB4). Due to inclusion of the two-body long-range correlations, we are able to obtain improved results for the ground-state properties, including the critical value of the anisotropy, as well as the full excitation spectrum which is difficult to calculate by using the localized approximation scheme alone.

The spin-1/2 antiferromagnetic *XXZ* Heisenberg Hamiltonian in terms of spin raising s^+ and lowering s^- operators is given by

$$H = \tfrac{1}{2}\sum_{\langle i,j\rangle}[s_i^+ s_j^- + s_i^- s_j^+ + 2\Delta s_i^z s_j^z], \qquad (1)$$

where Δ is the anisotropy and the sum on $\langle i, j\rangle$ runs over all the nearest-neighbor pairs once. The isotropic Heisenberg model is given by $\Delta = 1$. Classically, the ground state of equation (1) is ferromagnetic, with all spins aligned along the z-axis for all lattices when $\Delta \leq -1$; for $|\Delta| \leq 1$ it is antiferromagnetic for all bipartite lattices with all spins are aligned along some arbitrary direction in the xy-plane; for $\Delta \geq 1$ it is antiferromagnetic with spins aligned along ($\pm$) directions of the z-axis. The classical Néel ground state with all up-spins on one sublattice and all down-spins on the other is chosen to be the model state in our CCM calculation. In this paper, as before, we use index i to label sites of the down-spin sublattice and index j for the up-spin sublattice. It is useful to introduce a transformation for the local spin axes of one sublattice. This is achieved by rotating all up-spins by 180° around the y-axis and hence every spin of the system points down in the Néel model state with $s^z = -1/2$. This transformation is given by, for all j-sublattice operators,

$s^{\mp} = s^x \mp \mathrm{i}s^y \to -s^{\pm}$ and $s^z \to -s^z$. The Hamiltonian of equation (1) after the rotation is rewritten as

$$H = -\tfrac{1}{2}\sum_{\langle i,j\rangle}[s_i^+ s_j^+ + s_i^- s_j^- + 2\Delta s_i^z s_j^z]. \tag{2}$$

The ket and bra ground states of the CCM are given in terms of correlation operators S and $\tilde{S}$ respectively:

$$|\Psi\rangle = \mathrm{e}^S|\Phi\rangle, \qquad S = \sum_I \mathcal{S}_I C_I^\dagger, \tag{3}$$

$$\langle\tilde{\Psi}| = \langle\Phi|\tilde{S}\mathrm{e}^{-S}, \qquad \tilde{S} = 1 + \sum_I \tilde{\mathcal{S}}_I C_I, \tag{4}$$

where the model state $|\Phi\rangle$ is the rotated Néel state as mentioned earlier with all the spins pointing down, $C_I^\dagger$ and C_I are the so-called configurational creation and destruction operators, respectively, with the nominal index I labeling the multi-spin raising and lowering operators:

$$\sum_I \mathcal{S}_I C_I^\dagger = \frac{1}{(n!)^2}\sum_{n=1}^{N/2}\sum_{i_1,i_2\cdots i_n,j_1,j_2\cdots j_n} \mathcal{S}_{i_1,i_2\cdots i_n,j_1,j_2\cdots j_n} \times s_{i_1}^+ s_{i_2}^+ \cdots s_{i_n}^+ s_{j_1}^+ s_{j_2}^+ \cdots s_{j_n}^+, \tag{5}$$

$$\sum_I \tilde{\mathcal{S}}_I C_I = \frac{1}{(n!)^2}\sum_{n=1}^{N/2}\sum_{i_1,i_2\cdots i_n,j_1,j_2\cdots j_n} \tilde{\mathcal{S}}_{i_1,i_2\cdots i_n,j_1,j_2\cdots j_n} \times s_{i_1}^- s_{i_2}^- \cdots s_{i_n}^- s_{j_1}^- s_{j_2}^- \ldots s_{j_n}^-, \tag{6}$$

with the ket- and bra-state correlation coefficients $\mathcal{S}_I$ and $\tilde{\mathcal{S}}_I$ to be determined variationally as shown below. We note that the bra-state $\langle\tilde{\Psi}|$ and the ket-state $|\Psi\rangle$ are not manifestly Hermitian conjugate to one another. The normalization condition $\langle\tilde{\Psi}|\Psi\rangle \equiv \langle\Phi|\Psi\rangle \equiv \langle\Phi|\Phi\rangle \equiv 1$ is satisfied by construction. The ground-state Schrödinger equation, $H|\Psi\rangle = E_\mathrm{g}|\Psi\rangle$, can now be written as

$$\hat{H}|\Phi\rangle = E_\mathrm{g}|\Phi\rangle, \tag{7}$$

where the similarity-transformed Hamiltonian $\hat{H}$ can be written in terms of a series of nested commutations as

$$\hat{H} = \mathrm{e}^{-S}H\mathrm{e}^S = H + [H,S] + \frac{1}{2!}[[H,S],S] + \cdots. \tag{8}$$

The expectation value of an arbitrary operator $\mathcal{O}$ can be written as

$$\bar{\mathcal{O}} = \langle\tilde{\Psi}|\mathcal{O}|\Psi\rangle = \langle\Phi|\tilde{S}\mathrm{e}^{-S}\mathcal{O}\mathrm{e}^S|\Phi\rangle = \bar{\mathcal{O}}(\{\mathcal{S}_I, \tilde{\mathcal{S}}_I\}). \tag{9}$$

The correlation coefficients $\{\mathcal{S}_I, \tilde{\mathcal{S}}_I\}$ are determined variationally by the following equations:

$$\frac{\delta\bar{H}}{\delta\tilde{\mathcal{S}}_I} = 0 \Rightarrow \langle\Phi|C_I\mathrm{e}^{-S}H\mathrm{e}^S|\Phi\rangle = 0, \tag{10}$$

$$\frac{\delta\bar{H}}{\delta\mathcal{S}_I} = 0 \Rightarrow \langle\Phi|\tilde{S}\mathrm{e}^{-S}[H, C_I^\dagger]\mathrm{e}^S|\Phi\rangle = 0. \tag{11}$$

In the following we will consider a specific approximation, namely the SUB2 + LSUB4 scheme as defined earlier, by similar truncations in S and $\tilde{S}$.

2. The ground-state energy for the SUB2 + LSUB4 approximation scheme

As mentioned in section 1, the SUB2 approximation retains two-spin-flip configurations of all orders. In the SUB4 scheme, additional four-spin correlations are also included. We hence write the SUB4 ket-state operators as

$$S = \sum_{i,j}^{N/2} b_{i,j}s_i^+ s_j^+ + \tfrac{1}{4}\sum_{i_1,i_2,j_1,j_2}^{N/2} g_{i_1,i_2;j_1,j_2}s_{i_1}^+ s_{i_2}^+ s_{j_1}^+ s_{j_2}^+, \tag{12}$$

where $b_{i,j}$ and $g_{i_1,i_2;j_1,j_2}$ are the two-spin-flip and four-spin-flip correlation coefficients, respectively. The full SUB4 scheme equations were obtained before [11], but they are difficult to solve. Here we consider the SUB2 + LSUB4 scheme which retains ten local configurations as shown in figure 1, in additional to the other two-body high-order coefficients of the SUB2 scheme.

As described in general by equation (10), the SUB4 approximation consists of two sets of equations, the two-spin-flip and four-spin-flip equations. The two-spin-flip equations are given by

$$\langle\Phi|s_i^- s_j^-\mathrm{e}^{-S_{SUB4}}H\mathrm{e}^{S_{SUB4}}|\Phi\rangle = 0, \tag{13}$$

from which we obtain the subset of the SUB2 + LSUB4 approximation as

$$\sum_\rho\Big[(1 + 2\Delta b_1 + 2b_1^2 + G_1)\delta_{r,\rho} + 2(\Delta + 2b_1)b_r + G_2\delta_{r,\rho_{3a}} + G_3\delta_{r,\rho_{3b}} + \sum_{r'} b_{r'+\rho+\rho_0}b_{r-r'-\rho_0}\Big] = 0, \tag{14}$$

where ρ is the nearest-neighbor index vector with four possible values for a square lattice, ρ_0 is any one of them, the G_α with $\alpha = 1, 2, 3$ are defined as

$$G_1 = 2g_4^a + 2g_4^b + 4g_4^c + 8g_4^d, \qquad G_2 = g_4^b, \qquad G_3 = g_4^c + 2g_4^d, \tag{15}$$

and the ρ_3 are 2D vectors containing ρ with $\rho_{3a} = (3\rho_x, 0)$ and $\rho_{3b} = (2\rho_x, \rho_y)$. The four-spin-flip equations are similarly given by

$$\langle\Phi|s_i^- s_{i'}^- s_j^- s_{j'}^-\mathrm{e}^{-S_{SUB4}}H\mathrm{e}^{S_{SUB4}}|\Phi\rangle = 0, \tag{16}$$

from which we obtain the following four coupled equations:

$$4\Delta g_4^a - 4\Delta b_1^2 + 4b_1g_4^c + 8b_1g_4^a + 8b_1^2b_3^b - 4b_3^ag_4^c - 8b_3^bg_4^c - 8b_3^bg_4^d = 0, \tag{17}$$

$$5\Delta g_4^b - \Delta b_1^2 - 2\Delta b_1b_3^a + 8b_1g_4^b + b_3^ag_4^b + 2b_3^ag_4^d + 2b_1\,(b_3^a)^2 + 4b_1^2b_3^b + 4b_1b_3^ab_3^b - 6b_3^bg_4^d - 2b_5^cg_4^d - 2b_5^bg_4^d - 2b_5^bg_4^b - b_5^ag_4^b = 0, \tag{18}$$

$$5\Delta g_4^c - \Delta b_1^2 + 2b_1^3 - 2\Delta b_1b_3^b + 4b_1^2b_3^b + 4b_1\,(b_3^b)^2 + b_1g_4^a - b_3^ag_4^a + 8b_1g_4^c + 2b_1g_4^d - b_3^ag_4^d - 3b_3^bg_4^d - b_5^bg_4^d - b_5^cg_4^d - 2b_5^cg_4^c = 0, \tag{19}$$

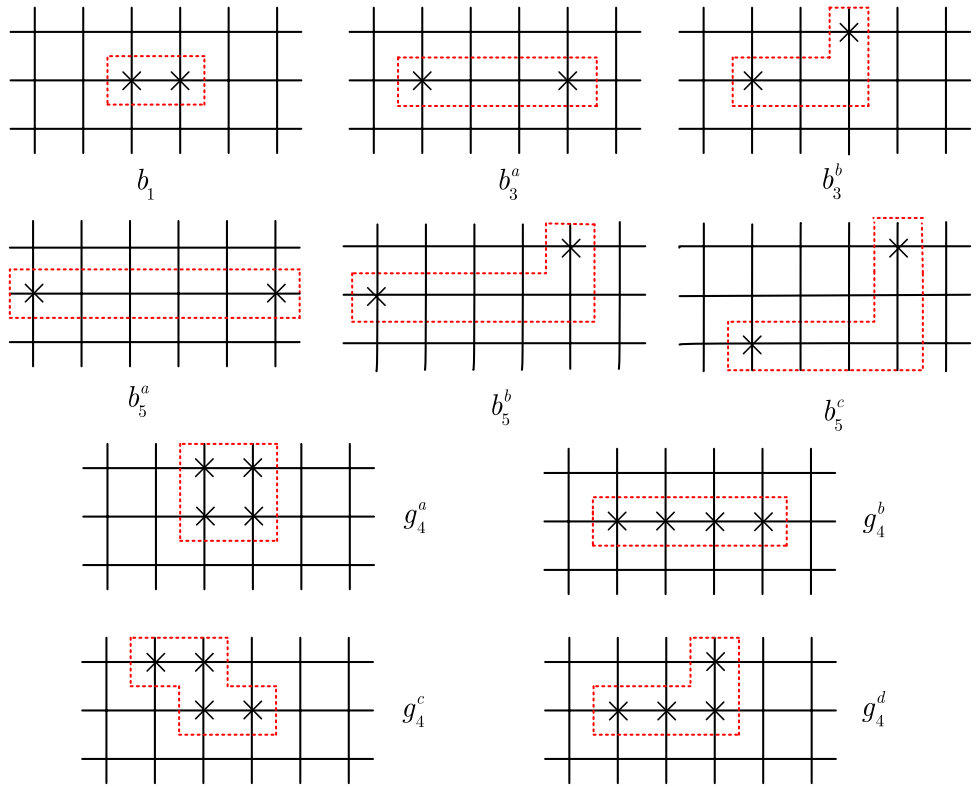

Figure 1. A graphical representation of the ten local configurations in equations (17)–(20) for the short-range part of the SUB2 + LSUB4 scheme. The flipped spins with respect to the Néel state are indicated by crosses.

$$
\begin{aligned}
&5\Delta g_4^d - \Delta b_1^2 - 2\Delta b_1 b_3^b + b_1^3 + b_1^2 b_3^a + 3b_1^2 b_3^b \\
&\quad + 4b_1 (b_3^b)^2 + b_1 b_3^b b_3^a + b_1 g_4^c + 8b_1 g_4^d - b_3^a g_4^d - b_3^b g_4^d \\
&\quad - 2b_5^c g_4^d - \tfrac{1}{2}(b_3^a g_4^c + 3b_3^b g_4^c + b_3^b g_4^b + b_3^a g_4^b \\
&\quad + b_5^c g_4^c + b_5^b g_4^c + b_5^c g_4^b + b_5^b g_4^b) = 0. \qquad (20)
\end{aligned}
$$

These nonlinear equations for the SUB2+LSUB4 scheme are solved firstly by Fourier transformation of equation (14) and then by an iteration method for equations (17)–(20). In particular, equation (14) becomes, after Fourier transformation,

$$
\begin{aligned}
&\gamma(\mathbf{q})\Gamma^2(\mathbf{q}) - 2K\Gamma(\mathbf{q}) + G_2\gamma_{3a}(\mathbf{q}) + G_3\gamma_{3b}(\mathbf{q}) \\
&\quad + (G_1 + 2b_1^2 + 2\Delta b_1 + 1)\gamma(\mathbf{q}) = 0, \qquad (21)
\end{aligned}
$$

which is easily solved with the physical solution,

$$\Gamma(\mathbf{q}) = \frac{K}{\gamma(\mathbf{q})}[1 - E(\mathbf{q})], \qquad (22)$$

where the constant K and the function $E(\mathbf{q})$ are given by, respectively,

$$K = \Delta + 2b_1, \qquad (23)$$

$$E(\mathbf{q}) = \sqrt{1 - k_1^2\gamma^2(\mathbf{q}) - k_2^2\gamma_{3a}(\mathbf{q})\gamma(\mathbf{q}) - k_3^2\gamma_{3b}(\mathbf{q})\gamma(\mathbf{q})}, \qquad (24)$$

and where $\gamma(\mathbf{q})$, $\gamma_{3a}(\mathbf{q})$ and $\gamma_{3b}(\mathbf{q})$ are defined, respectively, by

$$\gamma(\mathbf{q}) = \tfrac{1}{2}(\cos q_x + \cos q_y), \qquad (25)$$

$$\gamma_{3a}(\mathbf{q}) = \tfrac{1}{2}(\cos 3q_x + 1), \qquad (26)$$

$$\gamma_{3b}(\mathbf{q}) = \tfrac{1}{2}(\cos 2q_x + \cos q_y), \qquad (27)$$

with the constants k_1^2, k_2^2 and k_3^2 defined by

$$k_1^2 = \frac{1 + 2\Delta b_1 + 2b_1^2 + G_1}{(\Delta + 2b_1)^2}, \qquad k_2^2 = \frac{G_2}{(\Delta + 2b_1)^2}, \qquad k_3^2 = \frac{G_3}{(\Delta + 2b_1)^2}. \qquad (28)$$

In any approximation scheme of the CCM, the ground-state energy for the Hamiltonian of equation (2) is always given by [11]

$$E_g = \langle\Phi|\hat{H}|\Phi\rangle = -\frac{z}{8}N(2b_1 + \Delta), \qquad (29)$$

where z is the coordination number. In figure 2 and table 1, we present numerical results for the ground-state energy as a function of the anisotropy parameter Δ in our SUB2+LSUB4 scheme, together with those for the SUB2, SUB2 + g_4^a and LSUB4 schemes obtained earlier [11] for comparison. As can be seen, the SUB2 + LSUB4 results are lower than those of all of the other schemes. Furthermore, the critical value of the anisotropy $\Delta_c = 0.847$ beyond which the solution of equation (22) becomes imaginary is also improved and closer to the expected value of 1 than that of the SUB2 scheme (0.798) or that of the SUB2 + g_4^a scheme (0.818). In the high-order LSUBm scheme [16], the critical values are obtained as $\Delta_c = 0.763$ and 0.843 for $m = 6$ and 8, respectively, and $\Delta_c = 1$ after the extrapolation to $m = \infty$ is carried out. The corresponding values of Δ_c in the

Table 1. The ground-state energy per spin for the 2D spin-1/2 *XXZ* model in the SUB2 + LSUB4 scheme for some values of Δ, together with those for the full SUB2, SUB2 + g_4^a and LSUB4 schemes [11].

Δ	0.89	1	2	3	4	5
SUB2	−0.6118	−0.6508	−1.0807	−1.5547	−2.0413	−2.5331
SUB2 + g_4^a	−0.6189	−0.6561	−1.0816	−1.5550	−2.0414	−2.5332
LSUB4	−0.6162	−0.6636	−1.0831	−1.5555	−2.0418	−2.5333
SUB2 + LSUB4	−0.6289	−0.6641	−1.0832	−1.5555	−2.0416	−2.5333

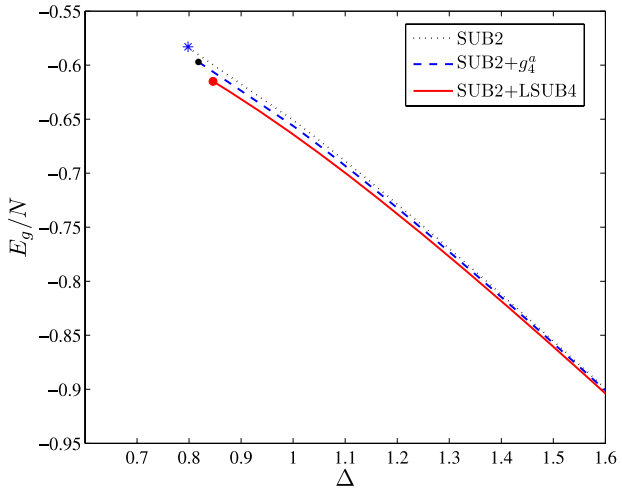

Figure 2. The ground-state energy per spin as a function of Δ for the spin-1/2 *XXZ* model in the full SUB2, SUB2 + g_4^a and SUB2 + LSUB4 schemes. The critical terminating points for each scheme are also indicated.

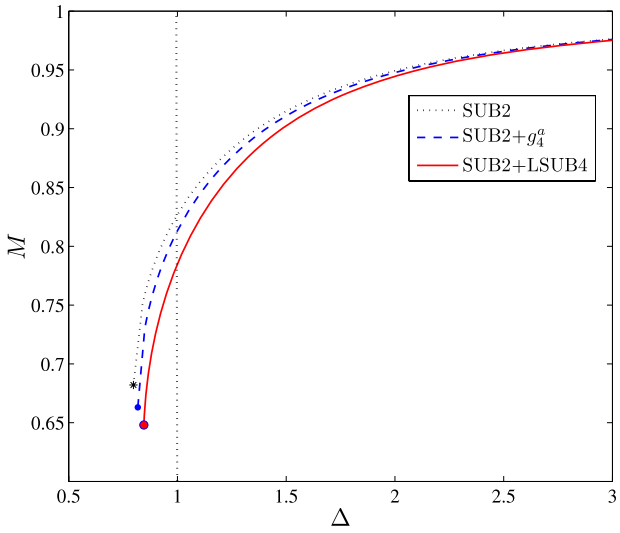

Figure 3. The staggered magnetization for the 2D spin-1/2 *XXZ* model for the full SUB2, SUB2 + g_4^a and SUB2 + LSUB4 schemes.

localized schemes are 0.637 in DSUB10 [19] and 0.766 in LPSUB5 [20]. The physics of this critical point was discussed in detail in [11].

3. Staggered magnetization

The staggered magnetization for a general spin quantum number s can be defined as

$$M = -\frac{1}{Ns}\langle\tilde{\Psi}|\sum_{l}^{N} s_l^z|\Psi\rangle, \tag{30}$$

where l runs over all the lattice sites for our rotated Hamiltonian of equation (2).

In the SUB2 + LSUB4 scheme we obtain

$$M = 1 - 2\sum_r \tilde{b}_r b_r - 2(\tilde{g}_{4\bar{4}}^a g_{4\bar{4}}^a + \tilde{g}_{4\bar{4}}^b g_{4\bar{4}}^b + \tilde{g}_{4\bar{4}}^c g_{4\bar{4}}^c + \tilde{g}_{4\bar{4}}^d g_{4\bar{4}}^d), \tag{31}$$

where two-body and four-body bra-state coefficients $\tilde{b}_r$ and $\tilde{g}_4$ are determined by the second variational equation (11). We solve these equations for the bra-state in similar fashion to those for the ket-state, namely by Fourier transformation for the two-body coefficients and by iteration methods for the four-body coefficients. We leave the details to the appendix and show the results in figure 3.

We find that at the critical Δ_c, $M_c = 0.649$ in our SUB2 + LSUB4 scheme, compared with $M_c = 0.663$ in the SUB2 + g_4^a scheme and $M_c = 0.682$ in the SUB2 obtained earlier [11]. Our SUB2 + LSUB4 result is in good agreement with $M = 0.6138$ from third-order spin-wave results [21], $M = 0.614$ from series expansion calculations [22] and $M = 0.615$ from quantum Monte Carlo calculations [23] at $\Delta_c = 1$. The higher-order LSUBm scheme with $m = 8$ produces $M = 0.705$ at $\Delta = 1$ before extrapolation and $M = 0.616$ after an extrapolation has been carried out [16]. The corresponding values of M at $\Delta = 1$ are 0.712 in the DSUB11 scheme [19] and 0.708 in the LPSUB6 scheme [20].

4. Spin-wave excitation spectra

The excited state in the CCM is given by applying an excitation operator X^e to the ket-state wavefunction,

$$|\Psi_e\rangle = X^e|\Psi_g\rangle = X^e e^S|\Phi\rangle, \tag{32}$$

where X^e in general is written in terms of the configurational creation operators $C_I^\dagger$ only as

$$X^e = \sum_I \chi_I^e C_I^\dagger, \tag{33}$$

with the excitation coefficient χ_I^e. From the Schrödinger equation $H|\Psi_e\rangle = E_e|\Psi_e\rangle$, it is straightforward to derive the following equation for the excitation coefficient:

$$\varepsilon_e \chi_I^e = \langle\Phi|C_I e^{-S}[H, X^e]e^S|\Phi\rangle, \tag{34}$$

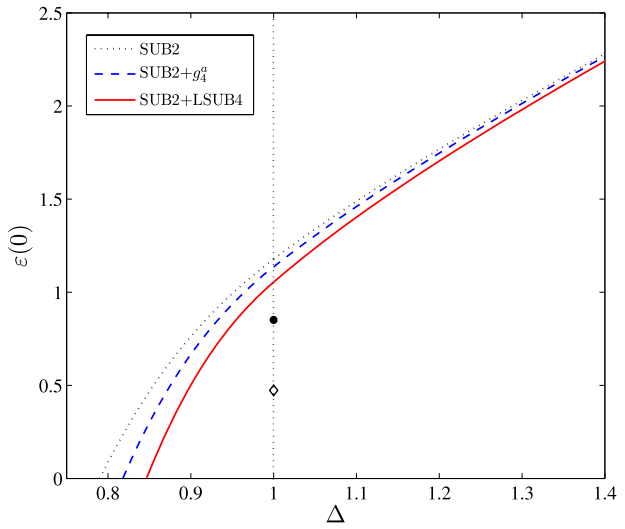

Figure 4. The excitation energy gap $\varepsilon(0)$ for the 2D spin-1/2 *XXZ* Heisenberg model as a function of Δ, for the full SUB2, SUB2 + g_4^a and SUB2 + LSUB4 schemes. The two gap values at $\Delta = 1$ are given by the LSUB4 scheme (•) and the LSUB8 scheme (◊) of [16] where the high-order excitation correlations are included as discussed in the text.

where $\varepsilon_e \equiv E_e - E_g$ is the excitation energy. Here, we consider the spin-wave excitations by including only a single spin-flip operator, $C_I^\dagger \simeq s_i^+$, like in the SUB2 scheme, as before [11]. After the Fourier transformation we obtain the energy spectrum in this linear approximation as

$$\varepsilon_e = \varepsilon(\mathbf{q}) = \tfrac{1}{2} zKE(\mathbf{q}), \tag{35}$$

where K and $E(\mathbf{q})$ are as defined before in equations (23) and (24), and z is the coordination number. We present the excitation gap, $\varepsilon(\mathbf{q})$ at $\mathbf{q} = 0$, as a function of Δ in figure 4. As can be seen from the figure, the energy gap in the SUB2 + LSUB4 scheme is smaller than that of the SUB2 and SUB2 + g_4^a schemes, implying that the energy gap is reduced in the higher-order approximations. For all these three schemes, the energy gap disappears at their corresponding critical anisotropy Δ_c. It is interesting to compare our results for the energy gap with those from the high-order LSUBm scheme [16]. At $\Delta = 1$ our SUB2 + LSUB4 gap value is $\varepsilon(0) = 1.05$ while the LSUB4 and LSUB8 values are much lower at $\varepsilon(0) = 0.851$ and 0.473 respectively. By employing an extrapolation, the LSUBm scheme produces an energy gap close to zero, corresponding to the SUB2 + LSUB4 result at the critical Δ_c. The much lower energy gap values away from the critical region from the higher-order LSUBm scheme are clearly due to the inclusion of higher-order correlations in the excitation operators, whereas we only include linear excitation operators in our calculations as given by equation (33) with $C_I^\dagger \simeq s_i^+$. However, our SUB2+LSUB4 scheme has the advantage of being capable of producing the full energy spectra due to inclusion of the long-range two-body correlations as discussed below.

In figure 5, we present our SUB2 + LSUB4 results for the spin-wave energy spectrum of equation (35) at Δ_c

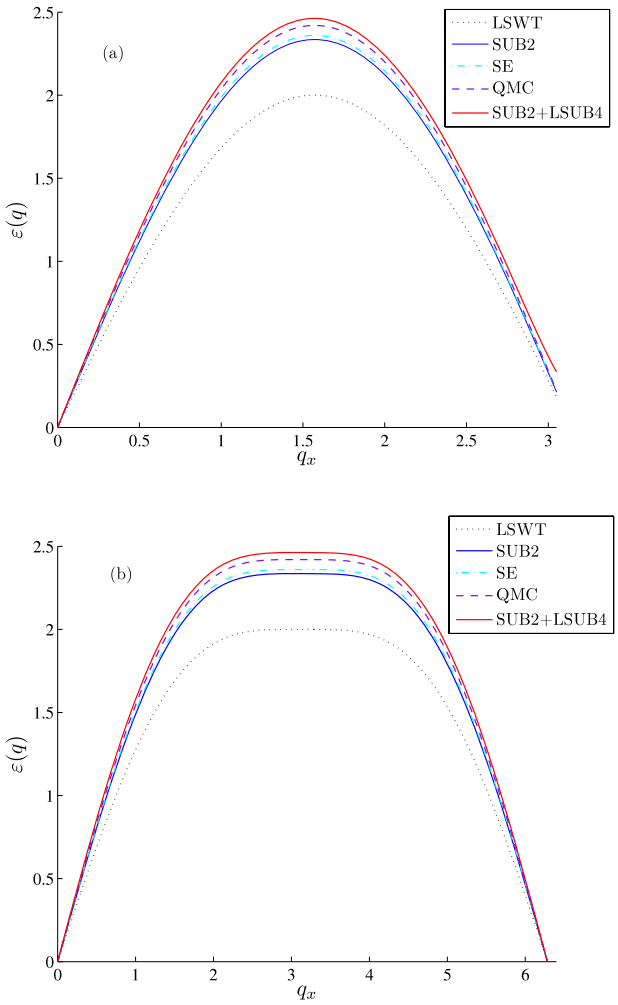

Figure 5. The spin-wave excitation spectra for the 2D spin-1/2 *XXZ* Heisenberg model at Δ_c for the CCM (SUB2 and SUB2 + LSUB4) results, and at $\Delta = 1$ for the linear spin-wave theory (LSWT), the series expansion (SE) [24] and quantum Monte Carlo calculations [25]. The energy spectra in (a) are for $q_y = 0$ and those in (b) are for $q_x = q_y$.

together with that from the SUB2 results [11], and at $\Delta = 1$, the results from linear spin-wave theory (LSWT), series expansion calculations (SE) [24] and quantum Monte Carlo calculations (QMC) [25]. The spin-wave velocity correction factor to the LSWT in our SUB2 + LSUB4 scheme is given by $K_c = 1.23$, in good agreement with 1.18 ± 0.02 from the SE and 1.21 ± 0.03 from the QMC calculations.

5. Summary and conclusion

In summary, we have obtained here numerical results for the ground-state energy, sublattice magnetization and excitation energy for the spin-half square-lattice antiferromagnetic *XXZ* model using the SUB2+LSUB4 scheme of the CCM. We find that our results for the ground-state properties in general are improved when compared with those obtained using the SUB2 or LSUB4 scheme alone. In particular, due to inclusion of the two-body long-range-order correlations, the SUB2 + LSUB4 scheme is capable of producing improved results around the

critical regions of the anisotropy, the excitation gaps at $\mathbf{q} = 0$ and the full spin-wave energy spectra. Good agreement for the spin-wave spectra is found with the high-order SE and the QMC calculations. This is in contrast to the case for the recent state-of-the-art calculations using the LSUBm scheme with computer algebra, where good results of the critical properties are obtained after an extrapolation to the limit $m \to \infty$ is carried out [16–20]. Away from the critical points, the long-range correlations are less important and the high-order LSUBm clearly provides better numerical results due to the inclusion of the high-order local correlations. We believe that the different approximation schemes in the CCM complement each other, yielding a more complete description of the physics of the spin–lattice Hamiltonian model, and in particular the SUB2 + LSUBm scheme as presented here has the advantage of producing the full excitation energy spectrum. Further improvement for the excitation energies away from the critical points can be obtained by including the higher-order local correlations in the excitations operator X^{e} as demonstrated in the LSUBm scheme of [16]. It will be interesting to apply our SUB2 + LSUBm scheme to other models such as the spin-1/2 XY model.

Acknowledgments

We are grateful to Professor R F Bishop and Dr D J J Farnell for useful discussion and assistance. M Merdan is also grateful to C Fullerton, R Morris, A Bladon, A Black and J Challenger for their help and support.

Appendix. The ground bra-state in the SUB2 + LSUB4 scheme

Similar to the ket-state equations, the bra-state ones in the SUB2 + LSUB4 scheme retain the two-body and four-body bra-state correlation coefficients defined as $\tilde{b}_r$, and $\tilde{g}_4^a$, $\tilde{g}_4^b$, $\tilde{g}_4^c$ and $\tilde{g}_4^d$, respectively. From equation (11), there are also two sets of equation for the bra-state coefficients. The first set is obtained by taking the partial derivatives of the Hamiltonian expectation $\bar{H}$ with respect to b_r, thus:

$$\frac{\partial \bar{H}}{\partial b_r} = \sum_{\rho}\Bigg[\Bigg(1 + a_1 + 2(\Delta + 2b_1)\tilde{b}_1 - 4\sum_{r'}\tilde{b}_{r'}b_{r'}\Bigg)\delta_{r,\rho} + a_3^a\delta_{r,\rho_{3a}} + a_3^b\delta_{r,\rho_{3b}} + a_5^a\delta_{r,\rho_{5a}} + a_5^b\delta_{r,\rho_{5b}} + a_5^c\delta_{r,\rho_{5c}} - 2(\Delta + 2b_1)\tilde{b}_r + 2\sum_{r'}\tilde{b}_{r'}b_{r-r'-\rho}\Bigg] = 0, \tag{36}$$

where the constants a_1, a_3^a, a_3^b, a_5^a, a_5^b and a_5^c are given as

$$\begin{aligned} a_1 &= \tilde{g}_4^b(-2\Delta b_1 - 2\Delta b_3^a + 2\,(b_3^a)^2 + 8b_1b_3^b + 4b_3^ab_3^b + 8g_4^b) + \tilde{g}_4^a(-8\Delta b_1 + 16b_1b_3^b + 8g_4^a + 4g_4^c) \\ &\quad + \tilde{g}_4^c(-2\Delta b_1 + 6b_1^2 - 2\Delta b_3^b + 8b_1b_3^b + 4\,(b_3^b)^2 + g_4^a + 8g_4^c + 2g_4^d) + \tilde{g}_4^d(-2\Delta b_1 + 3b_1^2 + 2b_1b_3^a \\ &\quad - 2\Delta b_3^b + 6b_1b_3^b + b_3^ab_3^b + 4\,(b_3^b)^2 + g_4^c + 8g_4^d), \end{aligned} \tag{37}$$

$$\begin{aligned} a_3^a &= -4\tilde{g}_4^ag_4^c + \tfrac{1}{2}\tilde{g}_4^d(2b_1^2 + 2b_1b_3^b - g_4^b - g_4^c - 2g_4^d) - \tilde{g}_4^c(g_4^a + g_4^d) + \tilde{g}_4^b(-2\Delta b_1 + 4b_1b_3^a \\ &\quad + 4b_1b_3^b + g_4^b + 2g_4^d), \end{aligned} \tag{38}$$

$$\begin{aligned} a_3^b &= \tilde{g}_4^a(8b_1^2 - 8g_4^c - 8g_4^d) + \tilde{g}_4^b(4b_1^2 + 4b_1b_3^a - 6g_4^d) + \tilde{g}_4^c(-2\Delta b_1 + 4b_1^2 + 8b_1b_3^b - 3g_4^d) + \tfrac{1}{2}\tilde{g}_4^d(-4\Delta b_1 \\ &\quad + 6b_1^2 + 2b_1b_3^a + 16b_1b_3^b - g_4^b - 3g_4^c - 2g_4^d), \end{aligned} \tag{39}$$

$$a_5^a = -\tilde{g}_4^bg_4^b, \tag{40}$$

$$a_5^b = -\tfrac{1}{2}\tilde{g}_4^d(g_4^b + g_4^c) - \tilde{g}_4^b(2g_4^b + 2g_4^d) - \tilde{g}_4^cg_4^d, \tag{41}$$

$$a_5^c = -\tfrac{1}{2}\tilde{g}_4^d(g_4^b + g_4^c + 4g_4^d) - \tilde{g}_4^c(2g_4^c + g_4^d) - 2\tilde{g}_4^bg_4^d \tag{42}$$

and where the 2D vectors are $\rho_{5a} = (5\rho_x, 0)$, $\rho_{5b} = (4\rho_x, \rho_y)$ and $\rho_{5c} = (3\rho_x, 2\rho_y)$ with the nearest-neighbor vector index $\rho = (\rho_x, \rho_y)$.

The second set of equations for the bra-state are obtained by taking the partial derivatives for $\bar{H}$ with respect to the four-body ket-state coefficients; hence,

$$\frac{\partial \bar{H}}{\partial g_4^a} = 2\tilde{b}_1 + \tilde{g}_4^a(4\Delta + 8b_1) + \tilde{g}_4^c(b_1 - b_3^a) = 0, \tag{43}$$

$$\frac{\partial \bar{H}}{\partial g_4^b} = 2\tilde{b}_1 + \tilde{b}_3^a + \tilde{g}_4^b(-b_5^a - 2b_5^b + 5\Delta + 8b_1 + b_3^a) - \tfrac{1}{2}\tilde{g}_4^d(b_5^b + b_5^c + b_3^a + b_3^b) = 0, \tag{44}$$

$$\frac{\partial \bar{H}}{\partial g_4^c} = 4\tilde{b}_1 + \tilde{b}_3^b + \tilde{g}_4^c(-2b_5^c + 5\Delta + 8b_1) + \tilde{g}_4^a(4b_1 - 4b_3^a - 8b_3^b) + \tfrac{1}{2}\tilde{g}_4^d\,(2b_1 - b_5^b - b_5^c - b_3^a - 3b_3^b) = 0, \tag{45}$$

$$\frac{\partial \bar{H}}{\partial g_4^d} = 8\tilde{b}_1 + 2\tilde{b}_3^b + \tilde{g}_4^b(-2b_5^b - 2b_5^c + 2b_3^a - 6b_3^b) + \tilde{g}_4^c(-b_5^b - b_5^c + 2b_1 - b_3^a - 3b_3^b) + \tilde{g}_4^d(-2b_5^c + 5\Delta + 8b_1 - b_3^a - b_3^b) - 8\tilde{g}_4^ab_3^b = 0. \tag{46}$$

Like in the solution of the ket-state coefficients, in order to find the bra-state correlation coefficients, we obtain the Fourier transformation of equation (36) which is solved together with equations (43)–(46) self-consistently. We rewrite equation (36) in the following simpler form:

$$\sum_{\rho}\Bigg[(1 + a_1 + 2K\tilde{b}_1 - 4\Xi)\delta_{r,\rho} + a_3^a\delta_{r,\rho_{3a}} + a_3^b\delta_{r,\rho_{3b}} + a_5^a\delta_{r,\rho_{5a}} + a_5^b\delta_{r,\rho_{5b}} + a_5^c\delta_{r,\rho_{5c}} - 2K\tilde{b}_r + 2\sum_{r'}\tilde{b}_{r'}\,b_{r-r'-\rho}\Bigg] = 0, \tag{47}$$

where K is again defined in equation (23) and the constant Ξ is given by

$$\Xi = \sum_{r'}\tilde{b}_{r'}b_{r'}. \tag{48}$$

After Fourier transformation, equation (47) reduces to

$$(1 + a_1 + 2K\tilde{b}_1 - 4\Xi)\gamma(\mathbf{q}) + A(\mathbf{q}) - 2K\tilde{\Gamma}(\mathbf{q}) + 2\gamma(\mathbf{q})\tilde{\Gamma}(\mathbf{q})\Gamma(\mathbf{q}) = 0, \tag{49}$$

where $\Gamma(\mathbf{q})$ and $\tilde{\Gamma}(\mathbf{q})$ are the Fourier transformations of the ket- and bra-state coefficients respectively, and the function $A(\mathbf{q})$ is given by

$$A(\mathbf{q}) = a_3^a\gamma_{3a}(\mathbf{q}) + a_3^b\gamma_{3b}(\mathbf{q}) + a_5^a\gamma_{5a}(\mathbf{q}) + a_5^b\gamma_{5b}(\mathbf{q}) + a_5^c\gamma_{5c}(\mathbf{q}),$$

with $\gamma_{3a}(\mathbf{q})$ and $\gamma_{3b}(\mathbf{q})$ as given before in equations (26) and (27) and new functions defined as

$$\gamma_{5a}(\mathbf{q}) = \tfrac{1}{2}(\cos 5q_x + 1),$$
$$\gamma_{5b}(\mathbf{q}) = \tfrac{1}{2}(\cos 4q_x + \cos q_y),$$
$$\gamma_{5c}(\mathbf{q}) = \tfrac{1}{2}(\cos 3q_x + \cos 2q_y).$$

Using the solution for $\Gamma(\mathbf{q})$ of equation (22) with the definition for $E(\mathbf{q})$ in equation (24), the physical solution of equation (49) for the bra-state is

$$\tilde{\Gamma}(\mathbf{q}) = \frac{D\gamma(\mathbf{q}) + 2A(\mathbf{q})}{4KE(\mathbf{q})}, \tag{50}$$

where the constant D is defined as

$$D = 2(1 + a_1 + 2K\tilde{b}_1 - 4\Xi). \tag{51}$$

The value of D can be determined self-consistently as follows. We first rewrite equation (48) as an integral in Fourier space as

$$\Xi = \frac{1}{\pi^2}\int_0^\pi \frac{1}{4}\left[D + \frac{2A(\mathbf{q})}{\gamma(\mathbf{q})}\right]\left[\frac{1}{E(\mathbf{q})} - 1\right] \mathrm{d}\mathbf{q}. \tag{52}$$

The bra-state coefficient $\tilde{b}_r$ is obtained by inverse Fourier transformation of $\tilde{\Gamma}(\mathbf{q})$:

$$\tilde{b}_r = \frac{1}{\pi^2}\int_0^\pi \mathrm{e}^{-\mathrm{i}r\cdot\mathbf{q}}\frac{D\gamma(\mathbf{q}) + 2A(\mathbf{q})}{4KE(\mathbf{q})}\mathrm{d}\mathbf{q}, \tag{53}$$

and, in particular, $\tilde{b}_1$ is given by

$$\tilde{b}_1 = \frac{1}{\pi^2}\int_0^\pi \frac{D\gamma^2(\mathbf{q}) + 2A(\mathbf{q})\gamma(\mathbf{q})}{4KE(\mathbf{q})}\mathrm{d}\mathbf{q}. \tag{54}$$

Combining equations (51), (52) and (54), we obtain the following expression for D:

$$D^{-1} = \frac{1}{c}\left[\frac{1}{\pi^2}\int_0^\pi \frac{1 - \gamma^2(\mathbf{q})/2}{E(\mathbf{q})}\mathrm{d}\mathbf{q} - \frac{1}{2}\right], \tag{55}$$

where the constant c is given by

$$c = I + a_1 + 1,$$

with the integral I defined as

$$I = \frac{1}{\pi^2}\int_0^\pi \left[\frac{A(\mathbf{q})\gamma(\mathbf{q}) - 2A(\mathbf{q})/\gamma(\mathbf{q})}{E(\mathbf{q})} + \frac{2A(\mathbf{q})}{\gamma(\mathbf{q})}\right]\mathrm{d}\mathbf{q}. \tag{56}$$

Using the above self-consistency equations for $\tilde{b}_1$, $\tilde{b}_3^a$, $\tilde{b}_3^b$, D and Ξ and by the iteration method, we obtain the numerical values for $\tilde{g}_4^a$, $\tilde{g}_4^b$, $\tilde{g}_4^c$ and $\tilde{g}_4^d$, the four-body bra-state coefficients. The staggered magnetization is then calculated by using equation (31).

References

[1] Coester F 1958 *Nucl. Phys.* **7** 421
[2] Čížek J 1966 *J. Chem. Phys.* **45** 4256
[3] Paldus J, Čížek J and Shavitt I 1972 *Phys. Rev.* A **5** 50
[4] Kümmel H, Lührmann K and Zabolitzky J 1978 *Phys. Rep.* **36** 1
[5] Bishop R and Lührmann K 1978 *Phys. Rev.* B **17** 3757
[6] Arponen J 1983 *Ann. Phys.* **151** 311
[7] Arponen J, Bishop R and Pajanne E 1987 *Phys. Rev.* A **36** 2539
[8] Bartlett R J 1989 *J. Phys. Chem.* **93** 1697
[9] Bishop R F 1991 *Theor. Chim. Acta* **80** 95
[10] Roger M and Hetherington J 1990 *Phys. Rev.* B **41** 200
[11] Bishop R F, Parkinson J B and Xian Y 1991 *Phys. Rev.* B **44** 9425
[12] Bursill R *et al* 1995 *J Phys.: Condens. Matter* **7** 8605
[13] Bishop R, Hale R and Xian Y 1994 *Phys. Rev. Lett.* **73** 3157
[14] Farnell D J J, Krüger S E and Parkinson J B 1997 *J. Phys.: Condens. Matter* **9** 7601
[15] Bishop R, Farnell D and Parkinson J 1998 *Phys. Rev.* B **58** 6394
[16] Bishop R F *et al* 2000 *J. Phys.: Condens. Matter* **12** 6887
[17] Farnell D, Gernoth K and Bishop R 2001 *Phys. Rev.* B **64** 172409
[18] Bishop R F, Li P, Farnell D J J and Campbell C E 2009 *Phys. Rev.* B **79** 174405
[19] Bishop R, Li P and Schulenburg J 2009 *J. Phys.: Condens. Matter* **12** 479
[20] Bishop R and Li P 2011 *Phys. Rev.* A **83** 042111
[21] Hamer C and Arndt P 1992 *Phys. Rev.* B **46** 6276
[22] Oitmaa J Z W and Hamer C J 1991 *Phys. Rev.* B **43** 8321
[23] Runge K 1992 *Phys. Rev.* B **45** 12292
[24] Singh R 1989 *Phys. Rev.* B **39** 9760
[25] Chen G, Ding H-Q and Goddard W 1992 *Phys. Rev.* B **46** 2933